JACS
JOURNAL OF THE AMERICAN CHEMICAL SOCIETY

ARTICLE

pubs.acs.org/JACS

Ruthenium Agostic (Phosphinoaryl)borane Complexes: Multinuclear Solid-State and Solution NMR, X-ray, and DFT Studies

Yann Gloaguen,[†,‡] Gilles Alcaraz,[*,†,‡] Alban S. Petit,[§] Eric Clot,[*,§] Yannick Coppel,[†,‡] Laure Vendier,[†,‡] and Sylviane Sabo-Etienne[*,†,‡]

[†]CNRS, LCC (Laboratoire de Chimie de Coordination), 205 Route de Narbonne, F-31077 Toulouse, France

[‡]Université de Toulouse, UPS, INPT, F-31077 Toulouse, France

[§]Institut Charles Gerhardt, CNRS 5253, Université Montpellier 2, cc 1501, Place Eugène Bataillon, 34095 Montpellier, France

Supporting Information

ABSTRACT: The reactivity of the (*o*-phosphinophenyl)(amino)borane compound $HB(N^iPr_2)C_6H_4(o\text{-}PPh_2)$ prepared from $Li(C_6H_4)PPh_2$ and $HBCl(N^iPr_2)$ toward the bis(dihydrogen) complex $RuH_2(H_2)_2(PCy_3)_2$ (**1**) was studied by a combination of DFT, X-ray, and multinuclear NMR techniques including solid-state NMR, a technique rarely employed in organometallic chemistry. The study showed that the complex $RuH_2\{HB(N^iPr_2)C_6H_4(o\text{-}PPh_2)\}(PCy_3)_2$ (**3**), isolated in excellent yield as yellow crystals and characterized by X-ray diffraction, led in solution to PCy_3 dissociation and formation of an unsaturated 16-electron complex $RuH_2\{HB(N^iPr_2)C_6H_4(o\text{-}PPh_2)\}(PCy_3)$ (**4**), with a hydride trans to a vacant site. In both cases, the (phosphinoaryl)(amino)borane acts as a bifunctional ligand through the phosphine moiety and a Ru−H−B interaction, thus featuring an agostic interaction.

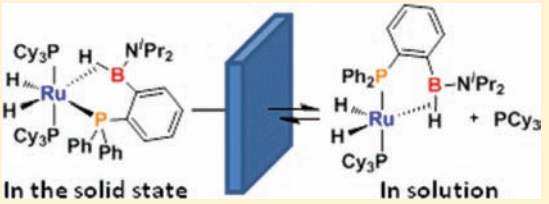

INTRODUCTION

The ability to accurately describe the bonding nature of ligands coordinated to a metal center has been facilitated by the increasingly sophisticated techniques available to chemists. In recent years, X-ray diffraction and DFT data in combination with multinuclear NMR studies enhanced understanding of a molecule's structure in the solid state and in solution. In the specific field of σ-complexes in which a σ bond of a ligand is coordinated to the metal center in a 3-center-2-electron mode, spectacular achievements have been made since the first report from Kubas et al. in 1984 of the coordination of dihydrogen to a metal center, without H−H bond breaking, leading to the unambiguous characterization of a σ-dihydrogen complex.[1,2] Seminal work was also conducted by Brookhart and Green in the early 1980s with the grounding of the concept of an agostic bond, that is to say, a ligand attached to a metal center via a 3-center-2-electron M−H−C interaction mode and a linker, thus making a distinct contrast with the corresponding σ-alkane complexes in which the alkane is bonded to the metal through the σ-C−H bond alone.[3] The recent example of the methane complex by Brookhart et al. is the prototypical example of a "true" σ-alkane complex.[4]

As regards boron chemistry, the use of tricoordinated borane compounds was a fruitful strategy to prepare σ-borane complexes as exemplified by the pioneering work of Hartwig et al. in 1996.[5] In this class of compounds, the HBR_2 borane is coordinated to the metal center via a σ-B−H bond. This class of compound is given the title "true" σ-borane to discriminate it from the Shimoi-type phosphine or amine−borane adducts (Figure 1).[6]

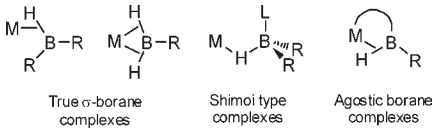

Figure 1. Various M−H−B coordination modes.

By comparison to the dihydrogen family, examples of "true" σ-borane complexes are still limited,[2] an occurrence that might be accounted for by the more challenging synthetic procedures that are required and by the tendency of dihydroborate ligation, especially when working with hydride systems.[7] Very recently, by adding monosubstituted boranes of general formula H_2BR to the bis(dihydrogen) complex $RuH_2(\eta^2\text{-}H_2)_2(PCy_3)_2$ (**1**), we have discovered a new type of bonding in which two geminal σ-B−H bonds are coordinated to the metal center.[8] A series of complexes of general formula $RuH_2(\eta^2{:}\eta^2\text{-}H_2BR)(PCy_3)_2$ was obtained with R = alkyl, aryl, amino.[9] The stabilization through two geminal B−H bonds allowed us to isolate the complex resulting from the first elementary step of dehydrogenation of ammonia borane, thus trapping the elusive aminoborane $H_2N{-}BH_2$.[9b] Preserving the tricoordinated mode at boron as a prerequisite,[10] we also launched a research program aimed at designing new bifunctional ligands to monitor the impact of the additional functional groups on the B−H activation mode.[11] Our first attempt allowed us to prepare the (diphenylphosphinomethyl)(diisopropylamino)borane, which

Received: May 5, 2011
Published: September 09, 2011

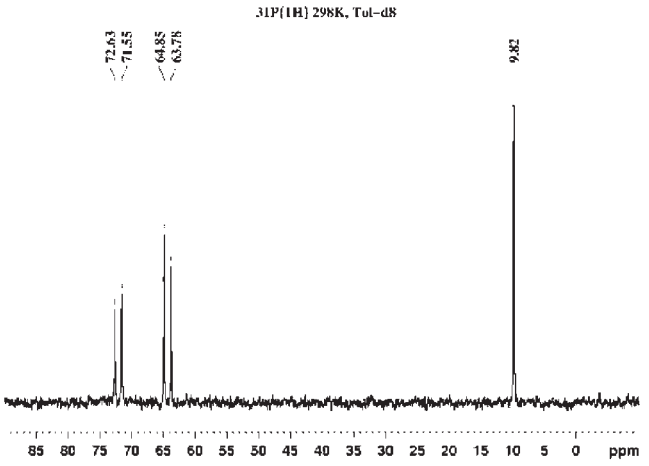

Figure 2. $^{31}P\{^{1}H\}$ NMR spectrum in C_7D_8 solution (202.537 MHz) of the crude reaction mixture at 298 K.

upon reaction with the bis(dihydrogen) complex **1** led to the isolation of the γ-B−H agostic complex $RuH_2\{HB(N^iPr_2)CH_2PPh_2\}(PCy_3)_2$ (**2**) resulting from the substitution of the two dihydrogen ligands and coordination of the borane compound through both phosphorus ligation and Ru−H−B interaction.[12] At this point, we want to emphasize our awareness that the term "agostic" should normally be reserved for a 3-center-2-electron M−H−C bond.[3a] The M−H−B interactions generally reported in the literature are common examples of 3-center-2-electron bonds, but involve a tetrahedral B_{sp3} atom, and are not encompassed by the term "agostic". However, in our systems as well as in the chromium complex reported by Braunschweig et al.,[13] in which the boron is kept trigonal, we believe that such a term better defines the interactions than the term "bridging hydrogen" currently employed for M−H−B bonds. We now describe our results concerning the synthesis and coordination at ruthenium, of a new (phosphinoaryl)borane compound $H-B(N^iPr_2)C_6H_4(o\text{-}PPh_2)$. Our study shows not only the tremendous influence the linker can have on the coordination, but also the benefits one can gain by combining solid-state and solution NMR techniques, at a moment when solid-state NMR is very much underutilized in organometallic chemistry.[14] Our detailed analysis by multinuclear solution and solid-state NMR, X-ray, and DFT data allows us to evidence a dynamic process and better define the nature of the "agostic" B−H bond.

RESULTS AND DISCUSSION

Synthesis and Properties of the (Phosphinophenyl)(amino)-borane Complexes 3 and 4. The (phosphinophenyl)(amino)-borane compound $H-B(N^iPr_2)C_6H_4(o\text{-}PPh_2)$ was isolated in good yield by addition of $(o\text{-}PPh_2)C_6H_4Li$ to $HBCl(N^iPr_2)$. It was fully characterized by multinuclear NMR and X-ray diffraction. The most important parameters are the singlet at −10.91 ppm and the broad signal at 38.4 ppm in the $^{31}P\{^{1}H\}$ and $^{11}B\{^{1}H\}$ NMR spectra, respectively. The X-ray diffraction structure determined at 110 K excludes any interaction between the boron and the phosphorus with a P···B distance higher than 3 Å (see Supporting Information, Figure S1). Location of hydrogen atoms by X-ray diffraction should be taken cautiously, but a great deal of progress has been made over the past decade, and in combination with DFT calculations, one can use the values involving the located hydrogens as, at least, additional

Scheme 1. Reaction of 1 with $HB(N^iPr_2)C_6H_4(o\text{-}PPh_2)$

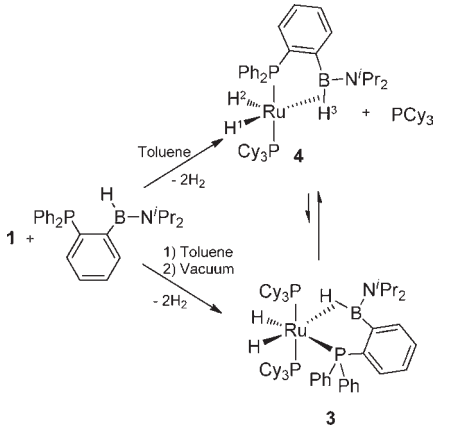

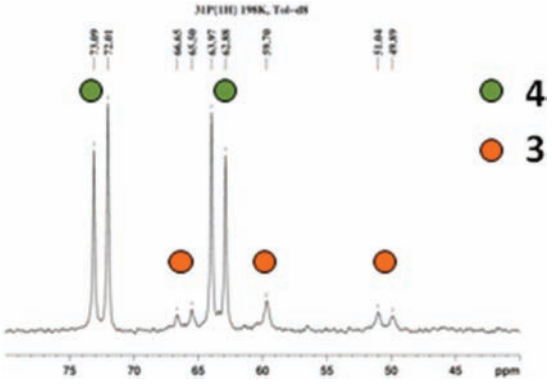

Figure 3. $^{31}P\{^{1}H\}$ NMR spectrum in C_7D_8 solution (202.537 MHz) of the crude reaction mixture at 198 K in the 40−80 ppm region.

parameters (see below).[15] Indeed, the hydrogen at boron could be located with a B−H distance of 1.076(10) Å, an interesting parameter to monitor the B−H bond activation upon coordination. By analogy with the reaction leading to the synthesis of $RuH_2\{H-B(N^iPr_2)CH_2PPh_2\}(PCy_3)_2$ (**2**),[12] we postulated that addition of 1 equiv of the new (phosphinoaryl)borane compound to the bis(dihydrogen) complex $RuH_2(\eta^2\text{-}H_2)_2(PCy_3)_2$ (**1**) should produce the new complex $RuH_2\{H-B(N^iPr_2)C_6H_4(o\text{-}PPh_2)\}(PCy_3)_2$ (**3**), corresponding to the substitution of the two dihydrogen ligands in **1** by the (phosphinoaryl)borane. However, we were quite surprised that NMR monitoring of the crude mixture led to clean spectra but not spectra accordant with the postulated species **3**. Indeed, as shown in Figure 2, the $^{31}P\{^{1}H\}$ NMR spectrum in C_7D_8 at room temperature shows two species: an AB pattern at δ 72.1 and δ 64.3 with a $^{2}J_{PP}$ coupling constant of 218 Hz, indicative of two different phosphorus in trans position, together with a singlet at δ 9.8 consistent with the formation of free PCy_3 in the mixture.

The ^{1}H NMR spectrum shows three signals of equal intensity in the hydride region. At 218 K, the two more shielded signals appear as a doublet of doublet of doublets at δ −25.69 and δ −12.67, whereas a broad signal is still observed at δ −6.41, but which sharpens upon ^{11}B decoupling. Selective irradiation led to complete assignment of the signals, and particularly a double selective irradiation $^{1}H\{^{11}B\}_{bb}\{^{31}P\}_{64.9}$ allows the measurement of a $^{2}J_{PPh2BH}$ coupling constant of 5 Hz between the two ends of the (phosphinoaryl)borane ligand (P and H^3, see Scheme 1).

dx.doi.org/10.1021/ja203828r |J. Am. Chem. Soc. 2011, 133, 17232–17238

The $^{11}B\{^1H\}$ NMR spectrum shows one broad resonance at δ 55 shifted to low field by comparison to the free (phosphinoaryl)-borane ($\Delta\delta$ = 17). These data are in agreement with the structure proposed for complex **4** in Scheme 1, and corresponding to an unsaturated 16-electron species $RuH_2\{H-B(N^iPr_2)C_6H_4-(o\text{-}PPh_2)\}(PCy_3)$.

Upon lowering the temperature below 238 K, the appearance of a broad ABM pattern in the $^{31}P\{^1H\}$ NMR spectrum was identified and is shown in Figure 3: AB resonances at 50.5 and 66.1 ppm with a large J_{PP} value of 233 Hz, and M resonance at 59.7 ppm (vide infra).

We monitored several crude reactions, and a postulated dynamic process consisting of phosphine dissociation from **3** and formation of **4** (vide infra) was consistently reproduced. By adding 10 equiv of PCy_3 to the reaction mixture, the postulated equilibrium could not be displaced, and the spectrum displayed in Figure 2 was observed yet again. In contrast, by using a very large excess of PCy_3, we could not detect any signal corresponding to an organometallic species, probably as a result of a decomposition pathway. However, when using ca. 40 equiv of PCy_3, NMR monitoring in the presence of an external reference showed at 195 K the decrease of the AB signal assigned to **4**. Complex **4** is the only organometallic species detected in solution at room temperature. We do need to lower the temperature bellow 238 K to start to detect **3** in solution as depicted in Figure 3 (spectrum run at 198 K, see also Figure S3). It was difficult to properly integrate the signals corresponding to **3** and **4**, but an equilibrium constant K_{eq} of ca. 3.7 could be estimated at 195 K, leading to a $\Delta_rG°$ value close to zero (ca. -2 kJ mol^{-1} at 195 K; see Supporting Information Figure S2). One can see from the $^{31}P\{^1H\}$ NMR variable temperature spectra (Supporting Information Figure S3) that when **3** could be detected, the two PCy_3 ligands of **3** appeared non equivalent and only one exchanged, with no average between free PCy_3 and **4**.

At 238 K, we were able to grow a few crystals, and the X-ray structure was determined at 110 K. The structure depicted in Figure 4 corresponds to the complex $RuH_2\{H-B(N^iPr_2)C_6H_4-(o\text{-}PPh_2)\}(PCy_3)_2$ (**3**), with ruthenium in a pseudo octahedral environment and two PCy_3 in trans positions, bent away from the (phosphinoaryl)borane ligand.

As can be seen from Table 1, the main geometrical parameters are essentially the same as those previously reported for complex **2** with the methylene spacer in place of the phenyl.[12] The main difference is a shorter Ru−B distance in **3** (2.503(3) Å). Comments on the parameters involving the hydrogen atoms will be found in the Computational Studies.

Upon dissolving the crystals of **3**, we observed the same $^{31}P\{^1H\}$ NMR spectrum featured in Figure 2. Consequently, it was thought pertinent to run a solid-state NMR spectrum of the orange powder obtained after addition of the (phosphinoaryl)-borane to **1** and immediate evaporation to dryness. The solid-state $^{31}P\{^1H\}$ NMR spectrum, recorded at room temperature and shown in Figure 5, displays exactly the same ABM pattern detected in solution at low temperature as shown in Figure 3 (AB resonances at 48.5 and 65.5 ppm with a large J_{PP} value of 233 Hz, and M resonance at 57.9 ppm). This is in agreement with a complex with two PCy_3 ligands (AB resonances) and one phosphinoarylborane ligand (M resonance).

The $^{11}B\{^1H\}$ solid-state NMR spectrum shows one complex signal depicted in Figure 6. Treatment of the signal and simulation with the program Dmfit allowed us to extract a chemical shift

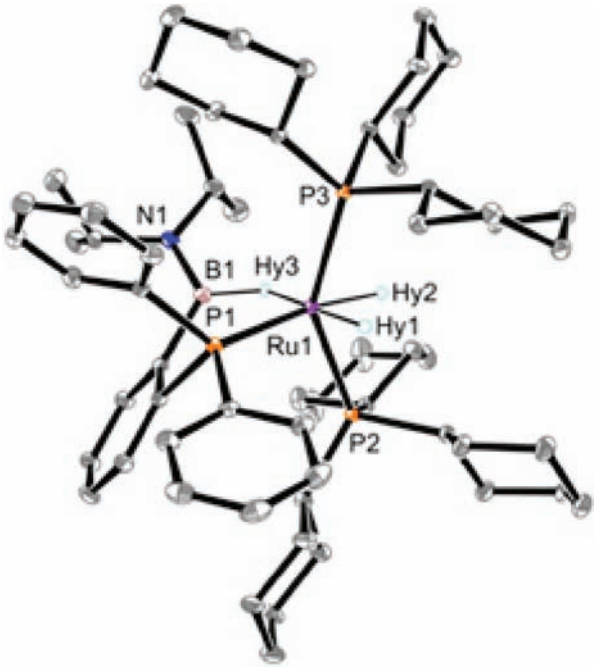

Figure 4. X-ray structure of **3**. Ellipsoids are shown at the 30% level. Hydrogens, except the hydrides, have been omitted for clarity.

Table 1. Selected Geometrical Parameters for the Experimental and Calculated (DFT/B3PW91) Structures of 3

	exp	calcd
Ru−P1	2.3350(6)	2.369
Ru−P2	2.3674(6)	2.412
Ru−P3	2.3265(6)	2.375
Ru···B	2.503(3)	2.551
B−N	1.419(3)	1.429
B−C8	1.600(4)	1.598
B−Hy3	1.22(3)	1.275
Ru···Hy3	1.79(3)	1.800
P1−Ru−P2	102.95(2)	103.1
P1−Ru−P3	107.91(2)	106.8
P2−Ru−P3	144.37(2)	145.6
P1−Ru−B	74.03(6)	74.2

at δ 57, thus in the same region as the signal observed for **4**. To validate our simulation, we treated free (phosphinoaryl)borane in a similar way (Figure 6) and obtained an identical value both in solution and in solid states (δ 38).

Remarkably, when C_7D_8 is added to the same sample in the same rotor and the $^{31}P\{^1H\}$ and $^{11}B\{^1H\}$ NMR spectra are run at room temperature in the same solid-state NMR AVANCE WB machine, the data indicate the formation of **4** as the sole ruthenium complex. Blank experiments with free PCy_3 were also performed to monitor the change of chemical shift in solution (δ 9.69) versus solid state (δ 7.6). Finally, the variable-temperature ^1H solution NMR spectra below 258 K showed, in addition to **4**, a new set of signals in agreement with the formulation of **3**: at 238 K, the hydride trans to the BH bond resonates as a pseudo doublet of triplets at δ −14.99 with $^2J_{PH}$ values of 15 and 20 Hz, consistent with its cis position to the three phosphorus

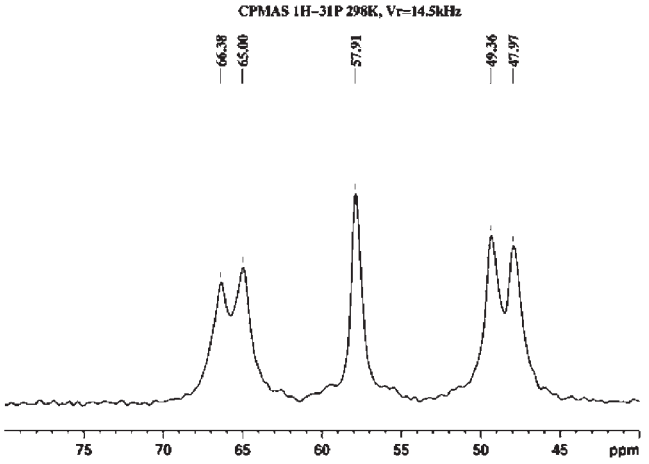

Figure 5. $^{1}H-^{31}P$ CP/MAS NMR spectrum in the solid state (161.768 MHz) of **3** at 298 K in the 40−80 ppm region.

entities; the hydride at δ −9.53 displays a large $^{2}J_{PH}$ value of 70 Hz, consistent with its trans position to the PPh_2 group; and the hydrogen connected to the boron resonates as a broad singlet at δ −8.11, the only signal sharpening upon ^{11}B decoupling. Separation of **4** from free PCy_3 proved difficult. However, upon dissolution of **3** in the presence of 1 equiv of $BH_3 \cdot THF$ and immediate evaporation to dryness, $BH_3 \cdot PCy_3$ was formed, allowing, after workup, the isolation of **4** as a brown powder contaminated by less than 10% of the tricyclohexylphosphine−borane adduct. Multinuclear NMR spectra of the powder, both in solution and in solid state, were in perfect agreement with the data described above.

Computational Studies. Density functional theory (DFT) calculations have been carried out to shed more light on the nature of the B−H agostic interaction in **3** and **4**, and on the energetic of the transformation **3** → **4** + PCy_3. The actual experimental systems **3**, **4**, and PCy_3 have been computed with the hybrid functional B3PW91. The calculated structure for **3** is in good agreement with the experimental data (Table 1). Albeit calculated as being longer than the experimental value (2.551 vs 2.503(3) Å), the Ru···B distance in **3** clearly indicates a stronger interaction of B−H with Ru as compared to that observed in **2** (2.7574(80) Å).[12] The calculated structure for **2** is in good agreement with experiment, and the Ru···B distance computed at 2.783 Å is consistent with a weaker B−H agostic interaction. This trend is further confirmed by the bond distances involving the hydrogen atom bonded to boron. The B−H bond is calculated as being longer in **3** than in **2** (1.275 and 1.244 Å, respectively); on the other hand, the Ru···H distance is calculated as being shorter in **3** than in **2** (1.800 and 1.891 Å, respectively). In both complexes, the B−H bond lies in the equatorial plane, but in the case of **2**, the B−H bond interacts mainly through the hydrogen atom, whereas in **3**, both atoms, H and B, participate to the agostic interaction. The B−H bond in **2** and **3** is elongated with respect to the calculated value in the free ligand (1.203 Å, CH_2; 1.202 Å, phenyl) essentially as a result of σ-donation from σ(B−H) to Ru. A Natural Bond Orbital (NBO) analysis[16] indicated that, in both complexes, the σ(BH) bond is more developed on the hydrogen atom (56.9%, **2**; 55.5%, **3**), and, therefore, the σ-donation induces a larger participation by the hydrogen atom. In the case of an agostic interaction with a less polar C−H bond, the interaction involves both atoms to a

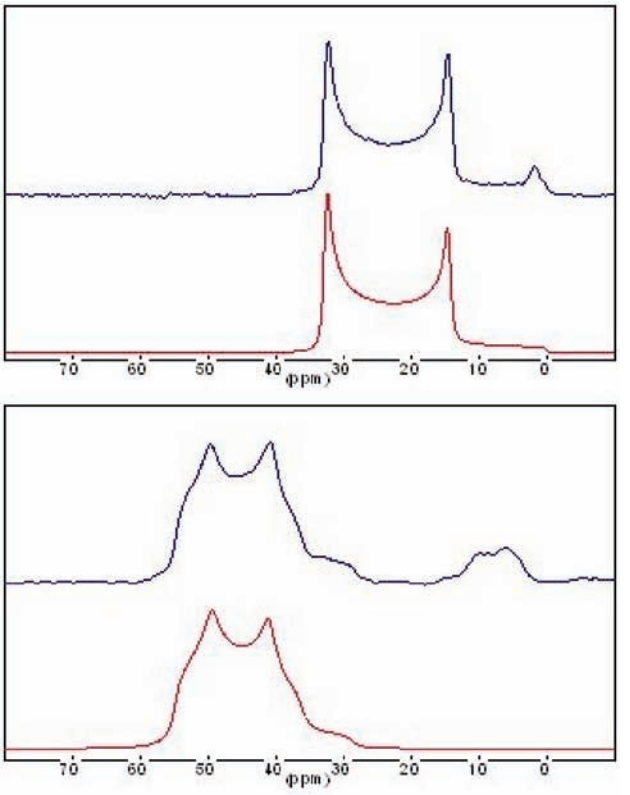

Figure 6. MAS $^{11}B\{^{1}H\}$ NMR spectra in the solid state (128.212 MHz) at 298 K. Top: The free (phosphinoaryl)borane $HB(N^{i}Pr_2)C_6H_4$-(*o*-PPh_2). Bottom: $RuH_2\{HB(N^{i}Pr_2)C_6H_4(o\text{-}PPh_2)\}(PCy_3)_2$ (**3**).

Table 2. Composition of the NLMO σ_{nlmo}(B−H) and LP_{nlmo}(Ru) Resulting from the Delocalization of the Parent NBO (σ(B−H) and LP(Ru)) into the Accepting NBO σ^*-(Ru−H) and LP*(B), Respectively

	σ_{nlmo}(BH)	LP_{nlmo}(Ru)
2	0.9586 σ(BH) + 0.2391 σ^*(RuH)	0.9569 LP(Ru) + 0.1017 LP*(B)
3	0.9407 σ(BH) + 0.2901 σ^*(RuH)	0.9570 LP(Ru) + 0.1553 LP*(B)
4	0.9297 σ(BH) + 0.3226 σ^*(RuH)	0.9356 LP(Ru) + 0.2385 LP*(B)

significant extent, leading to a geometry of interaction similar to that observed in **3**, but in contrast to that observed in **2**. However, in the present systems, the steric strain introduced by the tether in the phosphino∼borane ligand strongly influences the magnitude of the σ-donation. The population of the σ(BH) NBO is higher in **2** as compared to **3** (1.844 and 1.792 electron, respectively) as a result of less efficient σ-donation in the former. In addition, the more flexible nature of the hemilabile ligand in **3** allows for a better back-donation from Ru into the formally vacant p atomic orbital (AO) on boron. This electron transfer from Ru to B competes with π-donation from the nitrogen lone pair. The significantly longer B−N distance in **3** as compared to **2** (1.429 and 1.409 Å, respectively) indicates that π-donation from N is less efficient in the former as a result of increased back-donation from Ru. The latter interaction specifically shortens the Ru···B distance. Overall, both σ-donation from σ(BH) into σ^*(RuH) and back-donation from a nonbonding d orbital on Ru (LP(Ru)) into the vacant AO on B (LP*(B)) are stronger in **3** as a result of the more flexible nature of the ligand. This is nicely

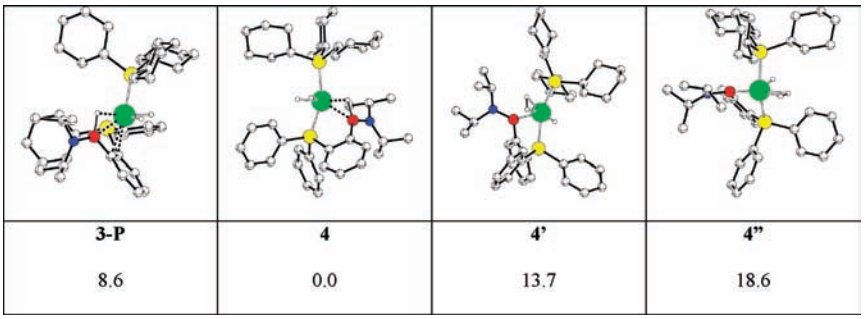

Figure 7. Optimized geometries for the 16-electron complexes **3-P**, **4**, **4′**, and **4″** and their relative energies (kcal mol^{-1}). Most H atoms omitted for clarity.

illustrated by the composition of the Natural Localized Molecular Orbitals (NLMO) corresponding to σ(BH) and LP(Ru) (Table 2).

To probe the energy landscape associated with the coordination of H−B(N^iPr_2)C_6H_4(*o*-PPh_2) to the $RuH_2(PCy_3)_2$ fragment, alternate isomers were optimized (Supporting Information). There is a clear energetic preference for the configuration observed experimentally for **3** with apical PCy_3 and the hydrides and the hemilabile ligand in the equatorial plane. In the solid-state structure of **3**, the Ru−P bond distances for the PCy_3 ligands are not equivalent (2.3265(6) and 2.3674(6) Å). To enhance the accepting capacity of the boron atom with respect to Ru, while keeping efficient donation from N, the phenyl tether expands toward one PCy_3 group, and the corresponding Ru−P bond is longer. This asymmetry is reproduced in the calculated structure for **3** (2.375 and 2.412 Å). The PCy_3 ligand "cis" to the phenyl tether is thus expected to be more labile. Optimization of a 16-electron complex, **3-P**, with a starting geometry similar to that of **3** deprived of the labile PCy_3 group yielded a local minimum featuring the phenyl tether weakly coordinated to Ru (Ru···C = 2.357 and 2.468 Å, see Figure 7).

This interaction introduces various geometrical modifications. The B−H bond is now perpendicular to the equatorial plane and is significantly more activated than in the 18-electron complex **3** (B−H = 1.298 Å, Ru···H = 1.752 Å, Ru···B = 2.237 Å). In addition, the PCy_3−Ru−PPh_2 angle has increased from 106.8° in **3** to 118.7° in **3-P**. The stronger B−H agostic interaction, the weak phenyl coordination, and the diminished trans influence of the hydride trans to PPh_2 are all stabilizing factors compensating for loss of Ru−PCy_3 bonding. Consequently, **3-P** + PCy_3 is only 6.3 kcal mol^{-1} less stable than **3**. Further increase of the P−Ru−P angle leads to a 16-electron complex more stable than **3-P** by 8.6 kcal mol^{-1}, with a geometry in agreement with the experimental observations of **4** (Figure 7). The calculated complex **4** features trans phosphines, a hydride trans to a vacant site, and an agostic B−H bond trans to the remaining hydride. The B−H bond is significantly activated (B−H = 1.313 Å, Ru···H = 1.771 Å, Ru···B = 2.256 Å).

The NBO analysis of the electronic structure of **4** indicated that the σ(BH) bond is less populated than in the 18-electron complex **3** (1.792 vs 1.742 electrons) as a result of stronger σ-donation in **4**. This is further confirmed by the expression of the NLMO for σ(BH) (Table 2) where the contribution of the accepting σ^*(RuH) orbital has increased from **3** to **4**. Additionally, the stronger agostic interaction in **4** results from stronger back-donation from Ru to boron as illustrated by the lengthening of the B−N bond (1.433 Å) and the expression for the NLMO of the ruthenium lone pair involved in the back-donation (Table 2). In addition, one methyl group of the N^iPr_2 group occupies the vacant site trans to the hydride, creating a very weak agostic interaction (Ru−C = 2.734 Å and Ru···H = 2.111 Å).[3a,17] B−H activation in **4** would result in dihydrogen hydrido−boryl complexes with either H (**4′**) or B (**4″**) trans to the vacant site (Figure 7). These two isomers have been computed and are less stable than **4** by 13.7 and 18.6 kcal mol^{-1}, respectively. By optimizing the relative positions of the various ligands in terms of stereoelectronic properties, the 16-electron complex **4** is computed to be more stable than **3** by −2.3 kcal mol^{-1}. Correction for basis set superposition effect (BSSE) has been taken into account using the counterpoise correction of Boys and Bernardi.[18] The BSSE-corrected relative energy between **3** and **4** is −6.9 kcal mol^{-1} in favor of **4**. So, even without any entropy correction associated with phosphine dissociation, the 16-electron complex **4** is more stable than the 18-electron complex **3**.

Not surprisingly for a dissociation process, the Gibbs free energy correction in the gas phase for the transformation **3** → **4** + PCy_3 amounts to −21 kcal mol^{-1}. There is no doubt that this value is overestimated by comparison to the NMR experimental determination. Following Ziegler,[19] when only ca. 50% of this correction is considered in solution, the Gibbs free energy difference between **3** and **4** is ca. −15 kcal mol^{-1} in favor of **4**. As complex **4** is already more stable than **3** electronically, entropy effects can only contribute to enhance its stability. This explains why the 16-electron complex **4** is the only compound observed at room temperature, and also why large excess of PCy_3 is necessary at low *T* to observe **3**.

■ CONCLUSIONS

By preparing a new phosphinoborane compound with a different spacer between the phosphine and the borane groups, phenyl versus methylene, we have demonstrated that the very recent examples of agostic borane complexes are more than mere curiosity, as it is possible to tune the B−H bond activation. In the case of the methylene spacer, the 18-electron complex **2** is stable in solution, whereas for the phenyl spacer, complex **3** undergoes a dissociative process, leading to free PCy_3 and formation of the corresponding 16-electron species **4**. Combination of various techniques is a prerequisite if one wants to better define the bonding nature in particular in complex systems. Here, we combine the widely routinized techniques of solution multinuclear NMR/DFT/X-ray with the more original tool of solid-state NMR. Together, the methods have enhanced understanding of the dissociative process. Computational studies have been very efficient for improving the definition of the B−H activation

level and to complement the structural data. We hope that this approach will encourage a large community to design strategies involving both solution and solid-state NMR techniques for improved understanding at a molecular level.

EXPERIMENTAL SECTION

All experiments were performed under a dry argon atmosphere using either Schlenck tube or glovebox techniques. Diethyl ether, THF, pentane, and toluene were obtained either from a solvent purification system MBraun SPS-800 Series or from distillation techniques under argon (refluxing over Na/benzophenone for diethylether and THF, over Na for toluene, and over CaH_2 for pentane). Deuterated NMR solvents were dried over molecular sieves (and over Na for THF-d_8), degassed by freeze−pump−thaw cycles, and stored under argon. The compounds (o-PPh_2)C_6H_4Li[20] and $RuH_2(\eta^2\text{-}H_2)_2(PCy_3)_2$ (**1**)[21] were prepared in accordance with published methods. NMR samples of sensitive compounds were all prepared in the glovebox, using NMR tubes fitted with Teflon septa. NMR spectra were obtained on Bruker AV 400 (^{1}H 400.13 MHz, ^{13}C 100.62 MHz, ^{11}B 128.38 MHz, ^{31}P 161.98 MHz) or AV 500 (^{1}H 500.33 MHz, ^{31}P 202.55 MHz, ^{11}B 160.53 MHz) spectrometers. Linear predictions of the FID from ^{11}B{^{1}H} spectra were made to extract the boron chemical shifts where necessary. Solid-state NMR experiments were recorded on a Bruker Avance 400 spectrometer equipped with a 4 mm probe. All MAS experiments were performed at ambient temperature. No corrections were made with respect to sample heating under MAS conditions. For ^{11}B MAS single pulse experiments, small flip angles of 1 μs for selective excitation of the central transition were used with recycle delay of 10 s. ^{31}P-CP/MAS spectra were recorded with a recycle delay of 5 s and a contact time of 3 ms. All of the ^{11}B and ^{31}P NMR spectra were recorded under high-power proton decoupling conditions. ^{11}B spectrum simulations were carried out using Dmfit program with the "Q mas 1/2" model. All chemical shifts for ^{1}H and ^{13}C are relative to TMS. ^{31}P and ^{11}B chemical shifts were referenced to external 85% H_3PO_4 and $BF_3\cdot Et_2O$ samples, respectively. Mass experiments were performed by the Mass Service of the University of Toulouse (Université Paul Sabatier). DCI technique (with CH_4) was used on a TSQ 7000 Thermo Electron apparatus. Elemental analyses were performed by the "in-house" service of the LCC, Toulouse. X-ray structures were recorded on a Bruker Kappa Apex II diffractometer using a graphite-monochromated Mo Kα radiation (λ = 0.71073 Å) and equipped with an Oxford Cryosystems Cryostream Cooler Device. Crystal data were collected at 110 K. All of the calculations have been performed with the Gaussian 09 package, at the B3PW91 level. See the Supporting Information for more details.

H−B(N^{i}Pr$_2$)C$_6$H$_4$(o-PPh$_2$). (o-PPh_2)C_6H_4Li (0.512 g, 1.908 mmol) was added to an ethereal solution (20 mL) of HBCl(N^{i}Pr$_2$) (0.360 g, 2.442 mmol) at −78 °C. The suspension was stirred for 30 min at this temperature and for 2 h at room temperature. Volatiles and solvent were then evaporated, and the crude mixture was dissolved in toluene. After filtration over Celite and removal of the solvent, a gum was washed with cooled pentane (−35 °C, 3 × 3 mL). H−B(N^{i}Pr$_2$)C_6H_4(o-PPh_2) was dried under vacuum and isolated as a white powder (78% yield). Data: ^{31}P{^{1}H} NMR (C_6D_6, 298 K, 161.99 MHz) δ −10.91. ^{11}B{^{1}H} NMR (C_6D_6, 298 K, 128.38 MHz) δ 38 (br). ^{1}H NMR (C_6D_6, 298 K, 400.13 MHz) δ 0.82 and 1.38 (d, 2 × 6H, $^3J_{HH}$ = 6.4 Hz, CH_3 ^{i}Pr), 3.12 and 3.87 (h, 2 × 1H, $^3J_{HH}$ = 6.4 Hz, CH ^{i}Pr), 5.95 (br, BH), 7.10−7.55 (m, 14H, CH_{ar}). ^{13}C{^{1}H} NMR (C_6D_6, 298 K, 100.62 MHz) δ 21.5 and 26.8 (s, CH_3 ^{i}Pr), 44.5 and 50.2 (s, CH ^{i}Pr), 127.4 (s, 1CH_{ar}), 128.0 (d, J_{PC} = 11.2 Hz, 1CH_{ar}), 128.3 (s, 2CH_{ar}), 128.5 (d, J_{PC} = 6.4 Hz, 2CH_{ar}), 130.2 (d, J_{PC} = 14.6 Hz, 1CH_{ar}), 132.8 (s, 1CH_{ar}), 134.6 (d, J_{PC} = 19.4 Hz, 2CH_{ar}), 138.4 (d, J_{PC} = 12.8 Hz, 2C_{IV}Ph), 140.6 (d, J_{PC} = 7.2 Hz, 1C_{IV}PhB), 150.6 (br, 1C_{IV}B). Anal. Calcd for $C_{24}H_{29}BNP$: C, 77.22; H, 7.83; N, 3.75. Found: C, 77.02; H, 7.82; N, 3.60. m/z = 373.28 (th), 374.22 (exp).

RuH$_2${H−B(N^{i}Pr$_2$)C$_6$H$_4$(o-PPh$_2$)}(PCy$_3$)$_2$ (3). A toluene (2 mL) solution of H−B(N^{i}Pr$_2$)C_6H_4(o-PPh_2) (400 mg, 1.072 mmol) was added to a toluene suspension (4 mL) of $RuH_2(\eta^2\text{-}H_2)_2(PCy_3)_2$ (**1**) (715.9 mg, 1.072 mmol) and stirred at room temperature for 1 min. After removal of the solvent, some pentane was added and then evaporated. This operation was repeated five times successively. After being dried under vacuum, a yellow orange powder was isolated in 95% yield. Suitable crystals of **3** were obtained after solubilization in a minimum amount of pentane and standing at −35 °C. Data for **3**: ^{31}P{^{1}H} NMR (Tol-d_8, 198 K, 202.54 MHz) δ 50.5 (d, $^2J_{PP}$ = 233 Hz, PCy_3), 59.7 (br, Ph_2P), 66.1 (d, $^2J_{PP}$ = 233 Hz, PCy_3). ^{31}P{^{1}H} NMR (solid state, 298 K, 202.54 MHz) δ 48.7 (d, $^2J_{PP}$ = 225 Hz, PCy_3), 57.9 (br, Ph_2P), 65.7 (d, $^2J_{PP}$ = 223 Hz, PCy_3). ^{11}B{^{1}H} (solid state, 298 K, MHz) δ 51 (after simulation). Anal. Calcd for $C_{60}H_{97}BNP_3Ru$: C, 69.48; H, 9.43; N, 1.35. Found: C, 69.66; H, 9.76; N, 1.11.

RuH$_2${H−B(N^{i}Pr$_2$)C$_6$H$_4$(o-PPh$_2$)}(PCy$_3$) (4). 48.2 μL of a 1 M solution of $BH_3\cdot$THF in THF (0.048 mmol) was added via syringe on a benzene solution of **3** (50 mg in 2 mL, 0.0482 mmol). All volatiles were immediately evaporated after addition and coevaporated with pentane. The crude was then dissolved in a minimum of pentane and kept at −35 °C overnight. A white precipitate could be separated, corresponding to the $PCy_3\cdot BH_3$ adduct. Solvent from the filtrate was then evaporated, and a brown powder was dried, containing mostly **4** contaminated with traces of the $PCy_3\cdot BH_3$ adduct. Data for **4**: ^{31}P{^{1}H} NMR (Tol-d_8, 298 K, 202.54 MHz) δ 72.1 (d, $^2J_{PP}$ = 218 Hz, Ph_2P), 64.3 (d, $^2J_{PP}$ = 218 Hz, PCy_3). ^{11}B{^{1}H} NMR (Tol-d_8, 298 K, 160.53 MHz) δ 55 (br). ^{1}H NMR (Tol-d_8, 218 K, 500.33 MHz) δ −25.69 (br, 1H, H^2), −12.67 (ddd, 1H, $^2J_{P1H}$ = 22.5 Hz, $^2J_{P2H}$ = 20.0 Hz, J_{H1H2} = 5.0 Hz, H^1), −6.41 (br, 1H, J_{P2H} = 5.0 Hz, H^3), −0.4 (br, 2 × 6H, CH_3 ^{i}Pr), 0.90−2.30 (m, 33H, Cy), 3.55 (br, 2 × 1H, CH ^{i}Pr), 6.9−7.5 (m, 10H, Ph), 7.66 (t, 2H, $^3J_{P1H}$ = 10.0 Hz, Ph), 7.86 (t, 2H, $^3J_{P1H}$ = 10.0 Hz, Ph). $T_{1\ min}$ (C_7D_8, 500.33 MHz) δ −25.69 (298 K, 330 ms), −12.67 (313 K, 352 ms), −6.41 (258 K, 138 ms). ^{13}C{^{1}H} NMR (C_6d_6, 298 K, 100.62 MHz) δ 21.0 (br), 23.0 (br), 24.5 (s), 24.9 (s), 26.8 (s), 27.0 (s), 27.3 (s), 27.9 (s), 28.1 (dd), 37.8 (s), 38.0 (s), 48.2 (br), 51.9 (s), 125.7 (d, J_{PC} = 5.0 Hz, CH_{ar}), 127.2 (d, J_{PC} = 9.1 Hz, CH_{ar}), 128.0 (pt, J_{PC} = 7.0 Hz, CH_{ar}), 128.3 (d, J_{PC} = 6.0 Hz, CH_{ar}), 129.1 (s, CH_{ar}), 129.3 (s, CH_{ar}), 129.4 (s, CH_{ar}), 129.7 (s, CH_{ar}), 133.1 (d, J_{PC} = 10.1 Hz, CH_{ar}), 134.3 (d, J_{PC} = 11.1 Hz, CH_{ar}), 134.9 (d, J_{PC} = 12.1 Hz, CH_{ar}), 138.9 (d, J_{PC} = 24.2 Hz, CH_{ar}), 143.5 (d, J_{PC} = 55.3 Hz, CH_{ar}), 146.2 (d, J_{PC} = 46.3 Hz, CH_{ar}), 158.8 (br, C_{IV}B).

ASSOCIATED CONTENT

Supporting Information. NMR data; computational details, Cartesian coordinates, and energy of the optimized structures; and X-ray data. The two crystal structures have been deposited at the Cambridge Crystallographic Data Centre and allocated the deposition numbers CCDC 817345 and 817346. This material is available free of charge via the Internet at http://pubs.acs.org.

AUTHOR INFORMATION

Corresponding Author

gilles.alcaraz@lcc-toulouse.fr; clot@univ-montp2.fr; sylviane.sabo@lcc-toulouse.fr

ACKNOWLEDGMENT

This work was supported by the CNRS and the ANR (Programme HyBoCat, ANR-09-BLAN-0184).

REFERENCES

(1) Kubas, G. J. *Chem. Rev.* **2007**, *107*, 4152–4205.

(2) Alcaraz, G.; Sabo-Etienne, S. *Coord. Chem. Rev.* **2008**, *252*, 2395–2409.

(3) (a) Brookhart, M.; Green, M. L. H.; Parkin, G. *Proc. Natl. Acad. Sci. U.S.A.* **2007**, *104*, 6908–6914. (b) Lein, M. *Coord. Chem. Rev.* **2009**, *253*, 625–634.

(4) Bernskoetter, W. H.; Schauer, C. K.; Goldberg, K. I.; Brookhart, M. *Science* **2009**, *326*, 553–556.

(5) Hartwig, J. F.; Muhoro, C. N.; He, X.; Eisenstein, O.; Bosque, R.; Maseras, F. *J. Am. Chem. Soc.* **1996**, *118*, 10936–10937.

(6) Shimoi, M.; Nagai, S.; Ichikawa, M.; Kawano, Y.; Katoh, K.; Uruichi, M.; Ogino, H. *J. Am. Chem. Soc.* **1999**, *121*, 11704–11712.

(7) Lachaize, S.; Essalah, K.; Montiel-Palma, V.; Vendier, L.; Chaudret, B.; Barthelat, J. C.; Sabo-Etienne, S. *Organometallics* **2005**, *24*, 2935–2943.

(8) Alcaraz, G.; Clot, E.; Helmstedt, U.; Vendier, L.; Sabo-Etienne, S. *J. Am. Chem. Soc.* **2007**, *129*, 8704–8705.

(9) (a) Gloaguen, Y.; Alcaraz, G.; Vendier, L.; Sabo-Etienne, S. *J. Organomet. Chem.* **2009**, *694*, 2839–2841. (b) Alcaraz, G.; Vendier, L.; Clot, E.; Sabo-Etienne, S. *Angew. Chem., Int. Ed.* **2010**, *49*, 918–920. (c) Alcaraz, G.; Chaplin, A. B.; Stevens, C. J.; Clot, E.; Vendier, L.; Weller, A. S.; Sabo-Etienne, S. *Organometallics* **2010**, *29*, 5591–5595.

(10) Alcaraz, G.; Grellier, M.; Sabo-Etienne, S. *Acc. Chem. Res.* **2009**, *42*, 1640–1649.

(11) Crabtree, R. H. *New J. Chem.* **2011**, *35*, 18–23.

(12) Gloaguen, Y.; Alcaraz, G.; Pécharman, A.-F.; Clot, E.; Vendier, L.; Sabo-Etienne, S. *Angew. Chem., Int. Ed.* **2009**, *48*, 2964–2968.

(13) Braunschweig, H.; Dewhurst, R. D.; Herbst, T.; Radacki, K. *Angew. Chem., Int. Ed.* **2008**, *47*, 5978–5980.

(14) (a) Duer, M. J. *Solid-State NMR Spectroscopy Principles and Applications*; Blackwell Science Ltd.: Cambridge, MA, 2002. (b) Rubio, M.; Suárez, A. s.; del Rìo, D.; Galindo, A. n.; Álvarez, E.; Pizzano, A. *Organometallics* **2008**, *28*, 547–560. (c) Walaszek, B.; Adamczyk, A.; Pery, T.; Yeping, X.; Gutmann, T.; Amadeu, N. d. S.; Ulrich, S.; Breitzke, H.; Vieth, H. M.; Sabo-Etienne, S.; Chaudret, B.; Limbach, H.-H.; Buntkowsky, G. *J. Am. Chem. Soc.* **2008**, *130*, 17502–17508. (d) Chierotti, M. R.; Gobetto, R. *Eur. J. Inorg. Chem.* **2009**, *2009*, 2581–2597. (e) Thibault, M.-H.; Lucier, B. E. G.; Schurko, R. W.; Fontaine, F.-G. *Dalton Trans.* **2009**, 7701–7716. (f) Rossini, A. J.; Mills, R. W.; Briscoe, G. A.; Norton, E. L.; Geier, S. J.; Hung, I.; Zheng, S.; Autschbach, J.; Schurko, R. W. *J. Am. Chem. Soc.* **2009**, *131*, 3317–3330. (g) Lucier, B. E. G.; Tang, J. A.; Schurko, R. W.; Bowmaker, G. A.; Healy, P. C.; Hanna, J. V. *J. Phys. Chem. C* **2010**, *114*, 7949–7962.

(15) Balcells, D.; Clot, E.; Eisenstein, O. *Chem. Rev.* **2010**, *110*, 749–823.

(16) Weinhold, F.; Landis, C. R. *Valency and Bonding: A Natural Bond Orbital Donor-Acceptor Perspective*; Cambridge University Press: Cambridge, U.K., 2005.

(17) Toner, A.; Matthes, J.; Gründemann, S.; Limbach, H.-H.; Chaudret, B.; Clot, E.; Sabo-Etienne, S. *Proc. Natl. Acad. Sci. U.S.A.* **2007**, *104*, 6945–6950.

(18) Boys, S. F.; Bernardi, F. *Mol. Phys.* **1970**, *19*, 553–566.

(19) Cooper, J.; Ziegler, T. *Inorg. Chem.* **2002**, *41*, 6614–6622.

(20) Higginson, B. R.; McAuliffe, C. A.; Venanzi, L. M. *Inorg. Chim. Acta* **1971**, *5*, 37–40.

(21) Borowski, A. F.; Sabo-Etienne, S.; Christ, M. L.; Donnadieu, B.; Chaudret, B. *Organometallics* **1996**, *15*, 1427–1434.